Electronic Supplementary Information (ESI)

Studies of Er(III)–W(V) compounds showing nonlinear optical activity and single–molecule magnetic properties

Kunal Kumar,[a] Olaf Stefanczyk,[a] Koji Nakabayashi,[a] Kenta Imoto[a] and Shin–ichi Ohkoshi*[a]

[a] *Department of Chemistry, School of Science, The University of Tokyo, 7–3–1 Hongo, Bunkyo–ku, Tokyo 113–0033, Japan.*
**Corresponding authors: ohkoshi@chem.s.u–tokyo.ac.jp*

LIST OF CONTENTS

1. Infrared spectroscopy of 1 – 3

In infrared spectra for all compounds, we can recognize three characteristic regions: 3700 - 2750 cm^{-1} corresponding to stretching bands of ν(O–H) from water (broad complex peak in 3700 - 2900 cm^{-1} range) and ν(C–H) from dma molecule (several sharp peaks in 3000 - 2750 cm^{-1} range); 2200 - 2100 cm^{-1} related to stretching bands ν(C≡N) of cyanide; and 1700 - 900 cm^{-1} (fingerprint region) consists of stretching band ν(C=O) of dma, bending bands δ(O–H) of water and several other bands δ(H–C–H), ν(N–C) and ν(C–C) from dma. Analysis of spectrum of $\{[Er^{III}(dma)_5][W^{V}(CN)_8]\}_n$ (**1**) confirms that assembly is anhydrous due to the absence of broad maximum around 3400 cm^{-1}, moreover, it also suggests that compound contains cyanido-bridges due to the fact that stretching bands of cyanide are shifted to higher energy (maximum around 2150 cm^{-1}) in respect to ionic systems $[Er^{III}(dma)_5(H_2O)_2]\cdot[W^{V}(CN)_8]\cdot dma\cdot H_2O$ (**2**) and $[Er^{III}(dma)_4(H_2O)_3]\cdot[W^{V}(CN)_8]\cdot dma\cdot 3H_2O$ (**3**) which is very well known effect polycyanidometallate complexes.[S1] It is worthy to emphasise that **2** and **3** have similar spectra which is a result of almost identical structure differing in the amounts of coordination and crystallization water and dma ligands.

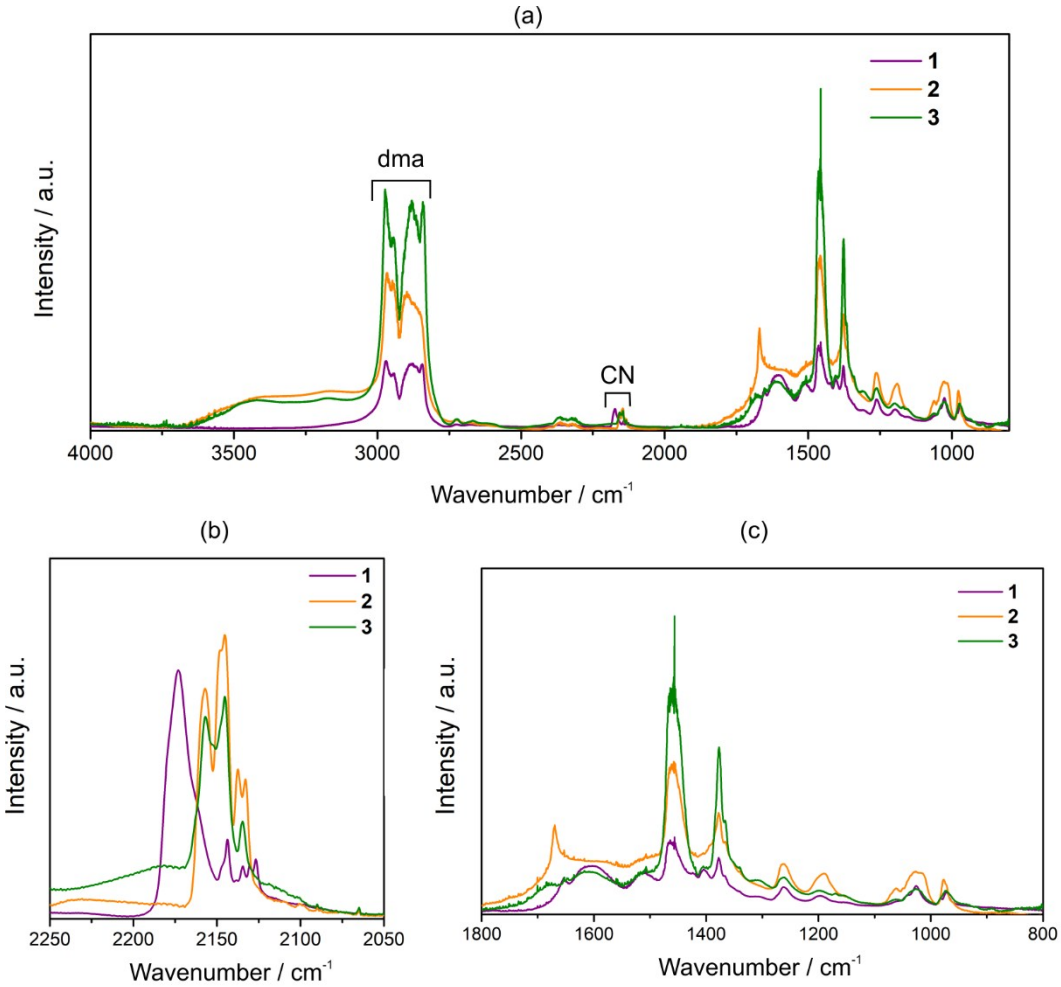

Figure S1. Infrared absorption spectra in nujol of **1** - **3** in (a) 4000 - 800 cm^{-1} (full range), (b) 2250-2050 cm^{-1} (CN stretching band region) and (c) 1800 - 800 cm^{-1} (fingerprint region).

2. Solid-state UV-Vis-NIR spectroscopy of 1 – 3

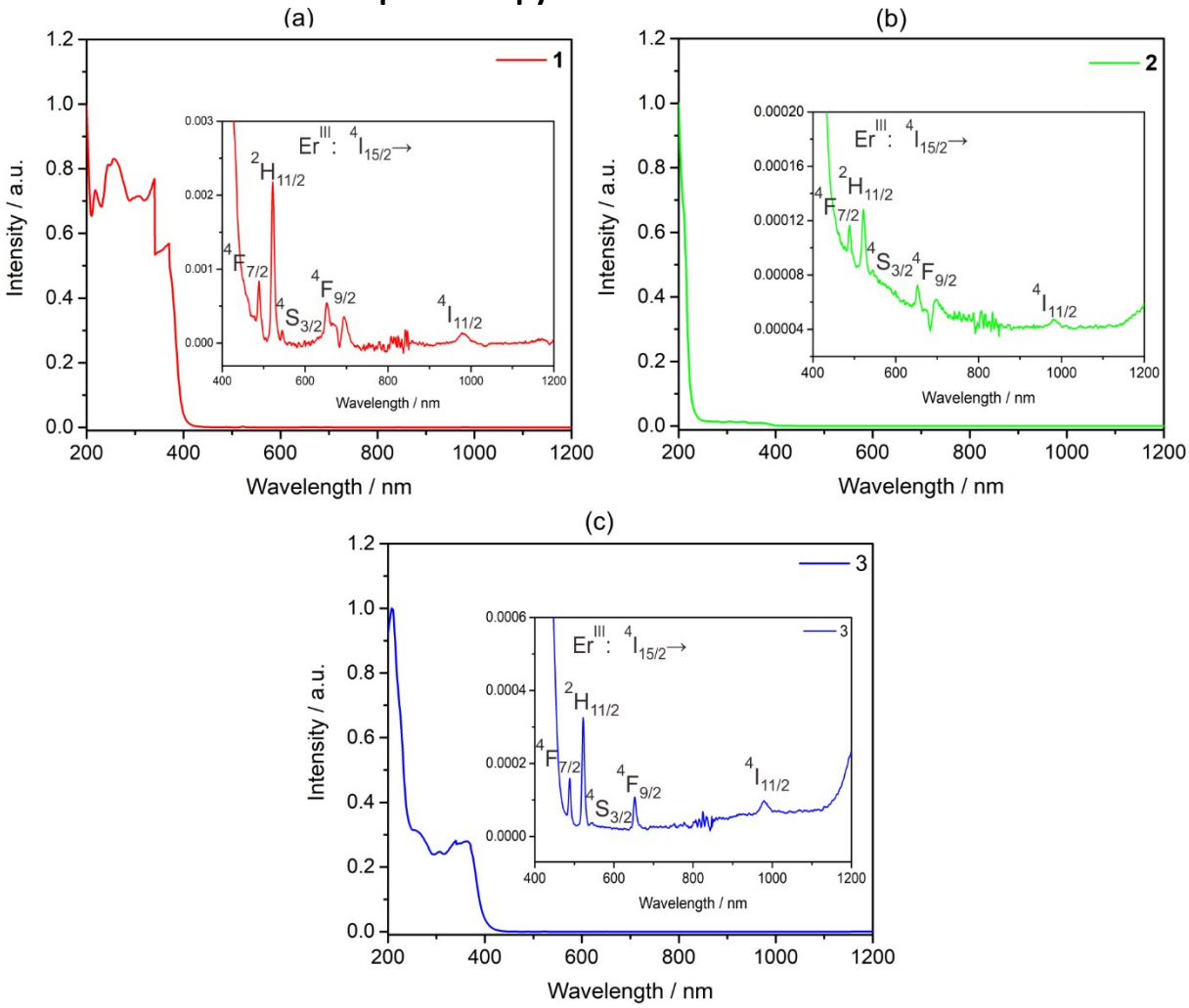

Figure S2. Room temperature solid–state UV–Vis–NIR absorption (Kubelka–Munk function) spectra of **1** - **3** (*a* – *c*, respectively) in 200 – 1200 nm range with indicated assignments.

3. Thermogravimetric analyses of 1 – 3

The cyanido–bridged complex **1** reveal no loss of solvent up to 130°C which is expected due to the fact that all of the dma molecules are coordinated to the Er^{III} ion. Further heating leads to decomposition of compound by releasing five dma molecules with 43.8% loss of weight at 224°C. In contrary to **1**, compounds **2** and **3** contain water and dma molecule as a crystalline unit which can be clearly seen in the TGA analysis in the first step of decomposition. Compound **2** starts to lose its solvents (one dma and three water molecule) in 50 – 65°C range which correspond to 12.41% mass loss. Upon further heating of **2**, the plateau can be seen up to 110°C and later 36.94% of weight loss is observed by 220°C due to release of five dma molecule. Raising the temperature above 220°C decomposes complex due to typical loss of cyanides. In case **3**, similar TGA pattern has been observed except the first step which correspond to 9.75% mass loss in 45 – 60°C range due to loss of six water molecule. Later it also losses its five dma molecule by 220°C which accounts for 37.87% weight lost with respect to initial mass. These observations in TGA plots additionally confirm the compositions of samples.

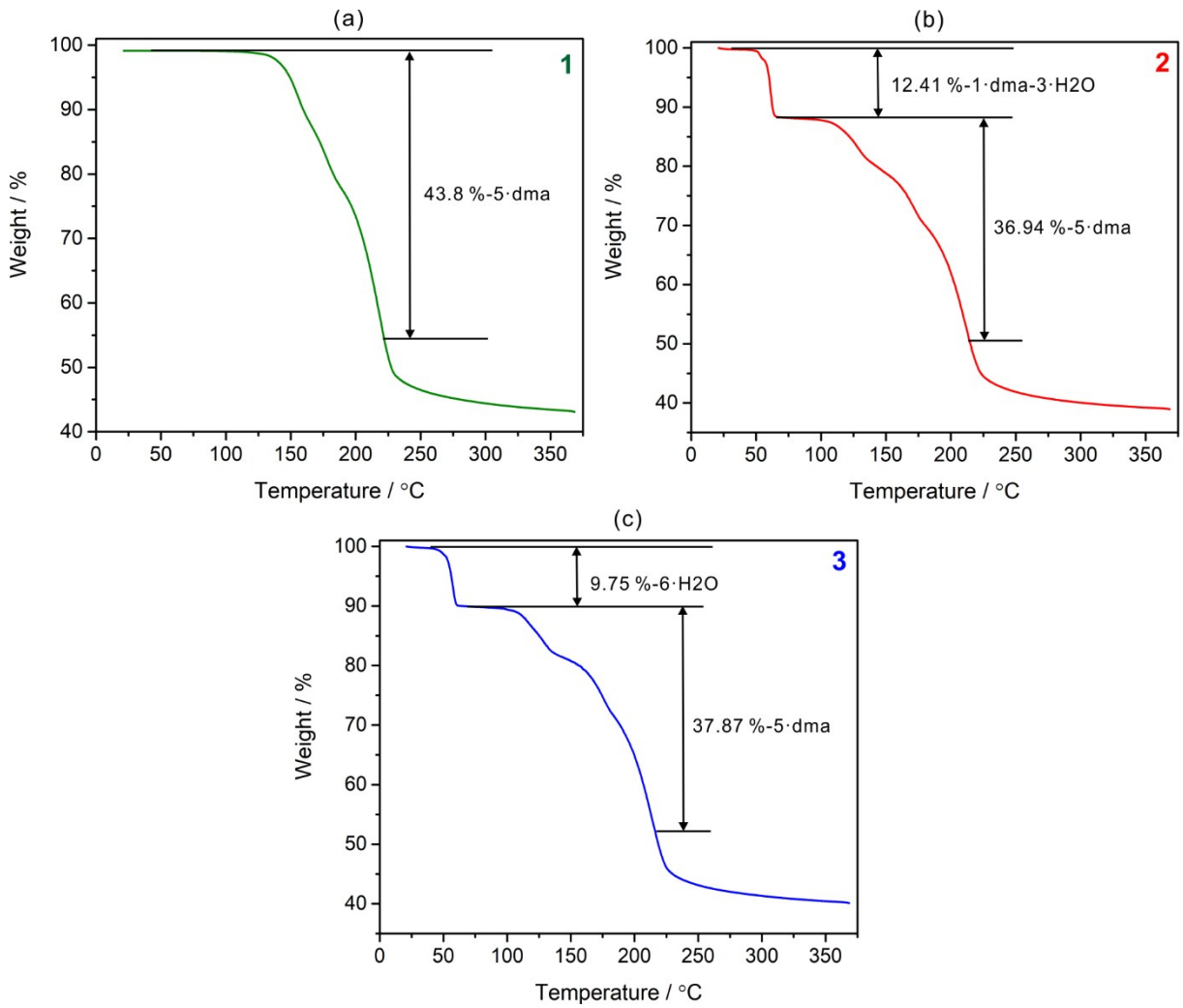

Figure S3. Thermogravimetric curves for powdered samples of **1** (*a*), **2** (*b*) and **3** (*c*) with indicated weight loss due to removal of solvent molecule.

4. Single crystal X-ray diffraction analyses of 1 – 3

Table S1. Single crystal X-ray diffraction data and structure refinement parameters for **1 – 3**.

Compound		1	2	3
Formula		$ErWC_{28}H_{45}N_{13}O_5$	$ErWC_{32}H_{60}N_{14}O_9$	$ErWC_{28}H_{51}N_{13}O_{11}$
M_W [g·mol^{-1}]		994.88	1136.04	1097.03
T [K]		90(2)	90(2)	90(2)
λ [Å]		0.71073 (Mo Kα)	0.71073 (Mo Kα)	0.71073 (Mo Kα)
Crystal system		monoclinic	monoclinic	monoclinic
Space group		$P2_1$ (#4)	$P2_1/n$ (#14)	$P2_1/c$ (#14)
Unit cell	a [Å]	9.7633(4)	9.8904(2)	9.6140(8)
	b [Å]	19.5696(8)	22.5488(5)	18.1609(12)
	c [Å]	10.4110(5)	20.4885(4)	25.5697(18)
	α [°]	90	90	90
	β [°]	109.168(8)	95.634(7)	98.033(7)
	γ [°]	90	90	90
V [Å^3]		1878.89(17)	4547.20(17)	4420.6(6)
Z		2	2	4
ρ_{calcd} (g/cm^{-3})		1.759	1.659	1.649
μ (mm^{-1})		5.329	4.422	4.548
F(000)		972	2256	2162
Crystal size [mm^3]		0.503×0.354×0.088	0.418×0.167×0.073	0.409×0.209×0.147
Crystal habit		plate	needle	needle
Θ range [deg]		3.04– 27.47	3.02– 27.48	3.06– 27.46
Index ranges		$-12 < h < 12$ $-25 < k < 25$ $-13 < l < 13$	$-12 < h < 12$ $-29 < k < 29$ $-26 < l < 26$	$-12 < h < 12$ $-22 < k < 23$ $-33 < l < 32$
Collected refls		17974	41500	42014
Unique refls		8389	10326	10110
R_{int}		0.0420	0.0925	0.0987
Completeness		99.7%	99.3%	99.8%
Data/restraints/ parameters		8389/61/528	10326/11/545	10112/0/570
GOF on F^2		1.101	1.068	1.002
Final R indices		R_1= 0.0338 [I>2σ(I)] wR_2 = 0.0536 (all)	R_1= 0.0764 [I>2σ(I)] wR_2 = 0.105 (all)	R_1= 0.0498 [I>2σ(I)] wR_2 = 0.1013 (all)
Largest diff peak/hole		1.168/-1.842 e·A^{-3}	2.104/-2.436 e·A^{-3}	1.269/-1.55 e·A^{-3}
Flack parameter		0.050(11)	---	---

Table S2. Detailed structure parameters of **1** – **3**.

Parameter	Distances (Å)			Parameter	Angles (°)		
	1	2	3		1	2	3
Er1–O1		2.340(5) [b]	2.337(4) [b]	**O5–Er1–O1**		69.03(17)	73.48(17)
Er1–O2	2.246(6) [a]	2.267(5) [a]	2.258(5) [a]	**O5–Er1–O3**		144.53(18)	141.75(17)
Er1–O3		2.327(5) [b]	2.352(4) [b]	**O5–Er1–O2**	152.2(3)	140.52(17)	145.22(17)
Er1–O4	2.221(6) [a]	2.275(5) [a]	2.331(5) [b]	**O5–Er1–O7**	78.8(2)	87.8(2)	96.46(19)
Er1–O5	2.257(6) [a]	2.284(5) [a]	2.210(4) [a]	**O5–Er1–O4**	80.7(2)	73.24(18)	70.42(18)
Er1–O6	2.260(6) [a]	2.198(5) [a]	2.202(5) [a]	**O1–Er1–O3**		145.85(17)	144.76(17)
Er1–O7	2.227(5) [a]	2.215(5) [a]	2.230(5) [a]	**O2–Er1–O1**		71.90(17)	72.55(16)
Er1–N1	2.452(8)			**O2–Er1–O3**		73.99(17)	72.57(16)
Er1–N3	2.472(8)			**O2–Er1–O4**	115.1(3)	146.21(18)	144.14(18)
W1–C1	2.173(9)	2.168(7)	2.176(7)	**O6–Er1–O5**	83.2(2)	98.5(2)	88.33(18)
W1–C2	2.159(8)	2.174(7)	2.170(7)	**O6–Er1–O1**		88.90(18)	93.82(17)
W1–C3	2.157(10)	2.172(7)	2.168(7)	**O6–Er1–O3**		90.4(19)	89.03(17)
W1–C4	2.173(9)	2.172(8)	2.167(7)	**O6–Er1–O2**	77.3(2)	86.02(18)	86.65(18)
W1–C5	2.145(8)	2.183(7)	2.171(7)	**O6–Er1–O7**	159.7(2)	173.46(19)	175.14(18)
W1–C6	2.177(9)	2.156(8)	2.172(7)	**O6–Er1–O4**	81.0(2)	87.06(19)	92.4(2)
W1–C7	2.157(8)	2.146(7)	2.178(8)	**O7–Er1–O1**		94.87(18)	88.35(18)
W1–C8	2.168(9)	2.173(7)	2.160(7)	**O7–Er1–O3**		83.48(18)	86.69(17)
W1–Er1 distance	5.753	7.416	7.621	**O7–Er1–O2**	115.6(2)	90.05(18)	89.85(19)
				O7–Er1–O4	105.2(2)	93.33(19)	88.5(2)
				O4–Er1–O1		140.97(18)	143.14(17)
				O4–Er1–O3		73.03(17)	71.58(18)
				N1–Er1–O4	158.8(3)		
				N1–Er1–O2	78.3(3)		
				N1–Er1–O5	80.9(2)		
				N1–Er1–O6	86.5(2)		
				N1–Er1–O7	81.4(2)		
				N1–Er1–N3	126.2(3)		
				N3–Er1–O2	72.9(2)		
				N3–Er1–O4	74.6(2)		
				N3–Er1–O5	134.9(2)		
				N3–Er1–O6	128.0(2)		
				N3–Er1–O7	72.2(2)		

[a] Parameter related to coordinated dma molecule. [b] Parameter related to coordinated water molecule.

Table S3. Results of Continuous Shape Measure (CShM) analyses of local geometry of Er(III) and W(V) centres for **1** – **3**.

Compound	Er^{III} centre			Compound	W^{V} centre		
	S_{PBPY-7}	S_{COC-7}	S_{CTPR-7}		S_{BTPR-8}	S_{SAPR-8}	S_{TDD-8}
ideal PBPY	0	8.582	6.675	ideal BTPR	0	2.262	2.709
ideal COC	8.582	0	2.007	ideal SAPR	2.267	0	2.848
ideal CTPR	6.675	2.007	0	ideal TDD	2.717	2.848	0
1	7.186	0.540	1.105	**1**	2.000	2.454	0.245
2	0.447	5.850	4.603	**2**	1.729	0.237	1.822
3	0.233	6.661	5.120	**3**	1.691	0.214	1.894

S_{PBPY-7} – the shape measure relative to the pentagonal bipyramid; S_{COC-7} – the shape measure relative to the capped octahedron; S_{CTPR-7} – the shape measure relative to the capped trigonal prism; S_{BTPR} – the shape measure relative to the bicapped trigonal prism; S_{SAPR} – the shape measure relative to the square

antiprism; S_{TDD} – the shape measure relative to the triangular dodecahedron; a smaller S – value reflects a better match with the ideal geometry (S = 0).[S2,S3]

5. Powder X–ray diffraction studies of 1 - 3

Calculated and simulated powder diffractograms for all compounds overlap almost perfect. The systematic shift of the diffraction peak positions between calculated and experimental patterns is due to the temperature effect as the single–crystal X–ray diffraction measurement was performed at 90 K, while the powder X–ray diffraction experiments at room temperature 298 K.

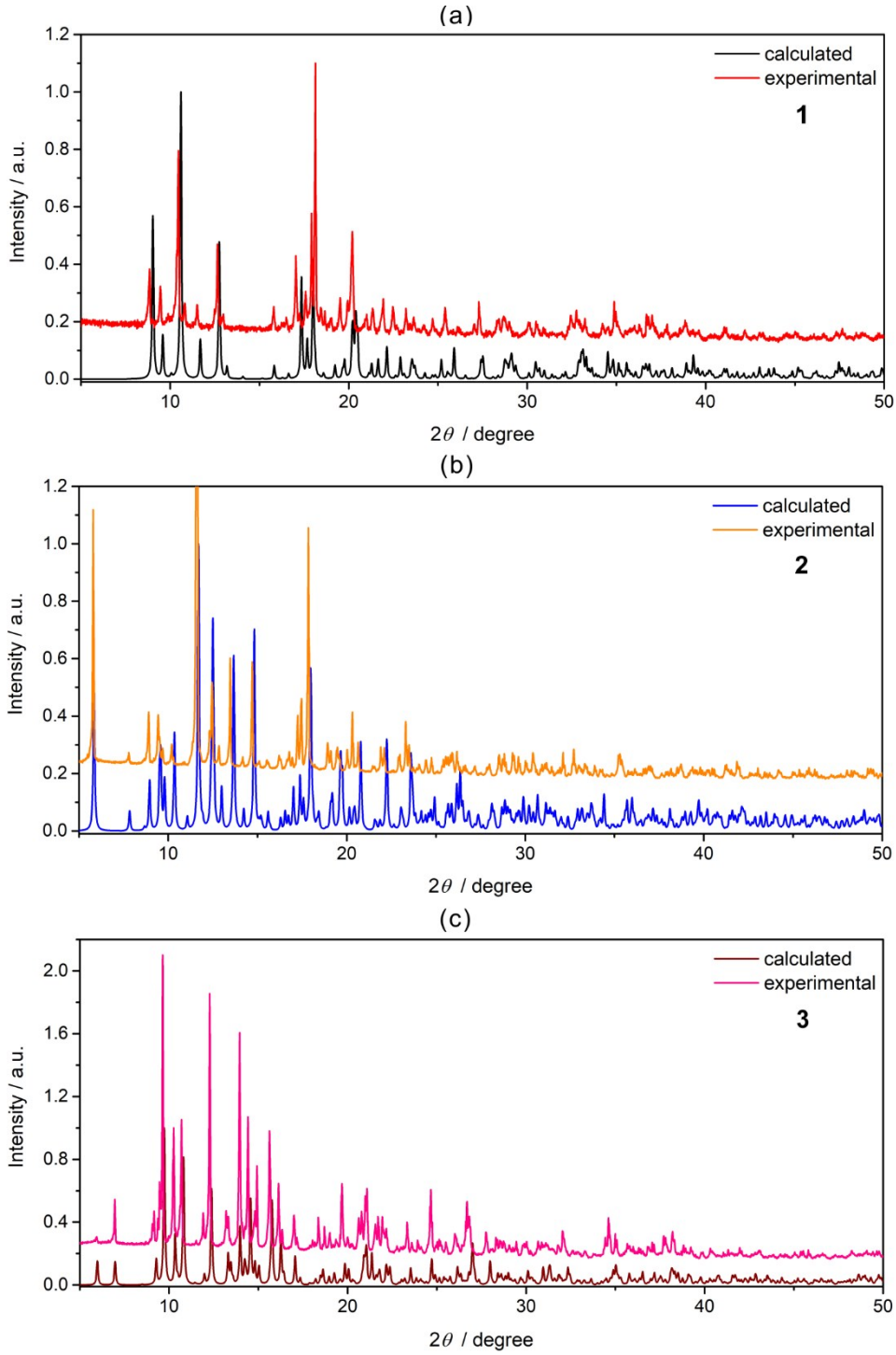

Figure S4. Experimental powder X–ray diffraction patterns of **1** – **3** compared with calculated ones for single crystal structures.

6. Second harmonic generation (SHG) studies of 1

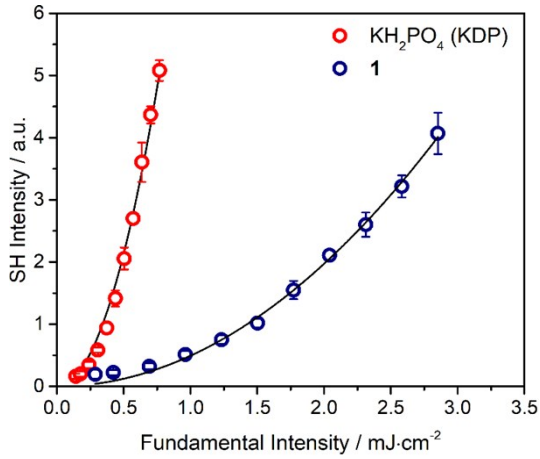

Figure S5. Second harmonic (SH) susceptibility of **1** compared with potassium dihydrogen phosphate (KDP).

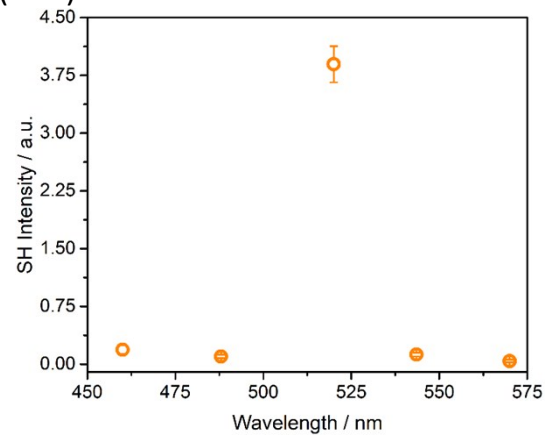

Figure S6. Second harmonic (SH) susceptibility of **1** plotted against wavelength to confirm the chromaticity aberration of SH signal.

7. Static magnetic studies of 1 - 3

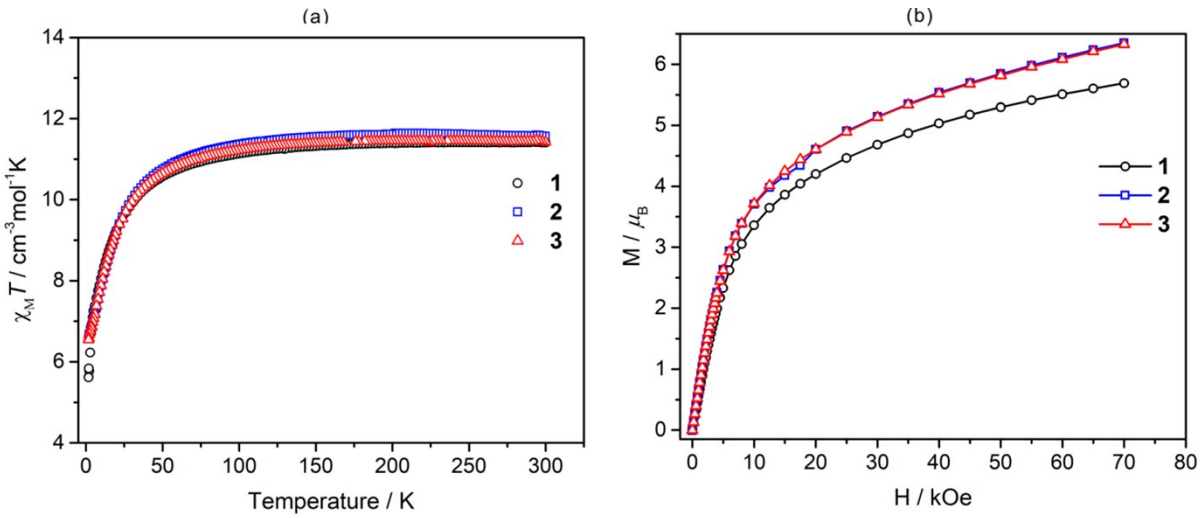

Figure S7. The *dc* magnetic properties of **1** – **3**: (a) temperature dependences of products molar magnetic susceptibility and temperature ($\chi_M T$) in H_{dc} = 1 kOe, and (b) magnetic field dependences of magnetization at T = 1.85 K.

8. Dynamic magnetic studies

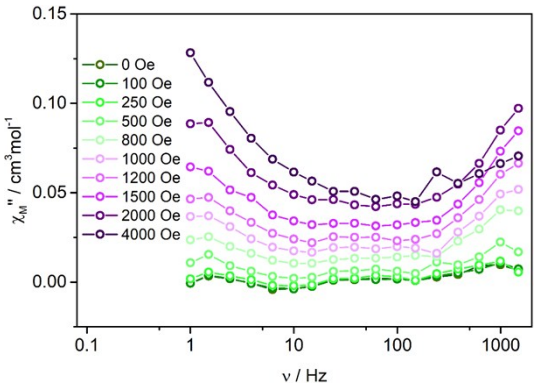

Figure S8. Frequency dependencies of out–of–plane χ_M" magnetic susceptibility of **1** in H_{ac} = 3 Oe at T = 1.85 K in various indicated *dc* magnetic fields. Solid lines are presented only to guide the eye.

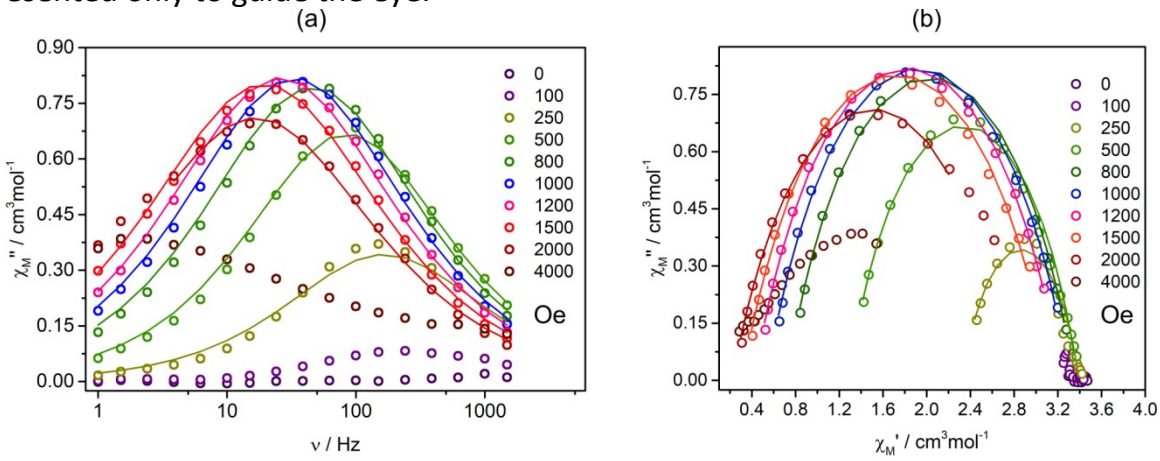

Figure S9. (a) Frequency dependencies of out–of–plane χ_M" magnetic susceptibility of **2** in H_{ac} = 3 Oe at T = 1.85 K in various indicated *dc* magnetic fields. (b) The related χ_M"–χ_M' Argand plots. Solid lines were fitted using the generalized Debye model (**Equation 1** and **2** in the manuscript).

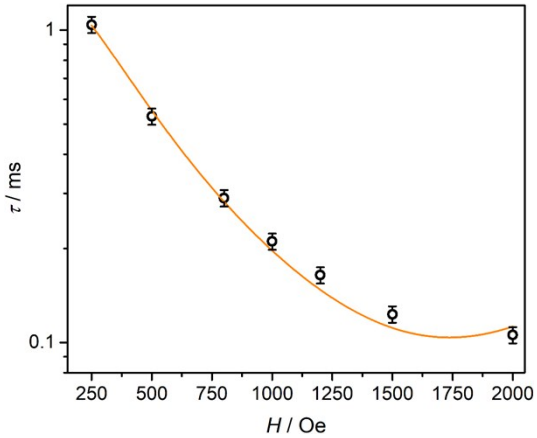

Figure S10. Ac magnetic-field-dependent relaxation time, τ, of **2** at T = 1.85 K, in H_{ac} = 3 Oe. The orange line is fitted using first two terms of **Equation 3** (equation is given in the manuscript).

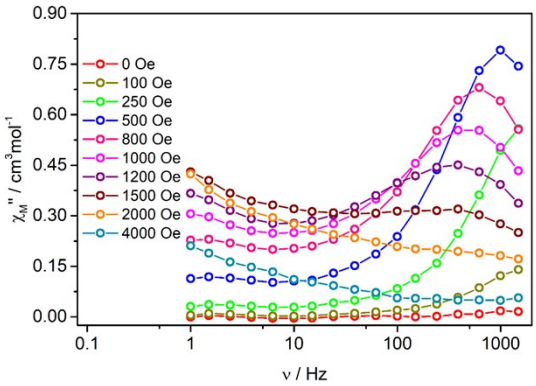

Figure S11. Frequency dependencies of out–of–plane χ_M" magnetic susceptibility of **3** in H_{ac} = 3 Oe at T = 1.85 K in various indicated *dc* magnetic fields. Solid lines are presented only to guide the eye.

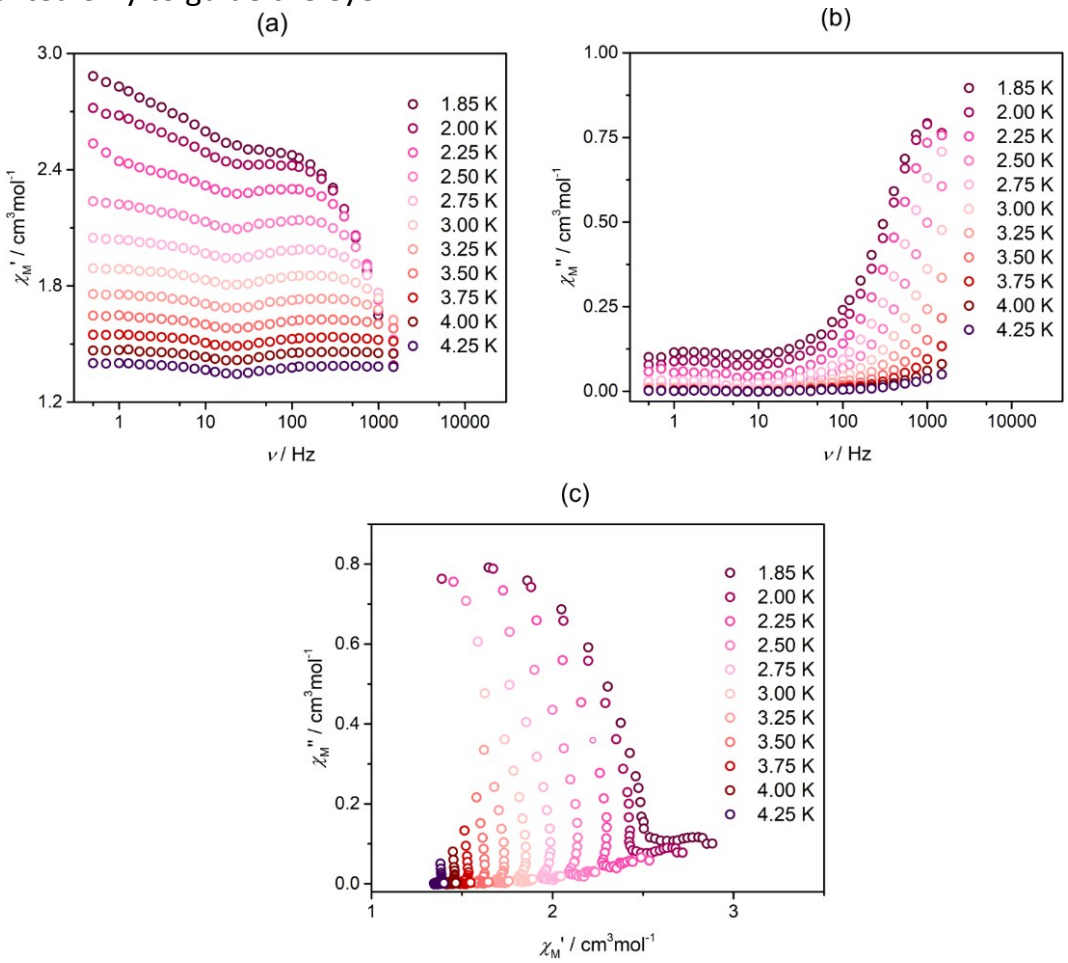

Figure S12. The *ac* magnetic characteristics of **3** in H_{dc} = 500 Oe and H_{ac} = 3 Oe: frequency (ν) dependences of the in–plane χ_M' (a) and out–of–plane χ_M" (b) components of the complex magnetic susceptibility for the indicated temperatures in 1.85 – 4.25 K range, and the related χ_M"–χ_M' Argand plots (c).

Table S4. Summary of ac magnetic data of **2**.

Magnetic field dependence of relaxation time[a]	
T **(K)**	1.85
A_{direct} **(s^{-1} K^{-1} Oe^{-4})**	$1.9(8)\cdot10^{-12}$
B_1 **(s^{-1})**	1456.8(5)
B_2 **(Oe^{-2})**	$6.5(3)\cdot10^{-6}$
Temperature dependence of relaxation time[b]	
H_{dc} **(Oe)**	1200
$\Delta E/k_B$ **(K)**	28.6(3)
τ_0 **(s)**	$9.8(1)\cdot10^{-8}$
B_{Raman} **(s^{-1} K^{-1})**	2.5(5)
n	5.04

[a] Result of fitting the field dependence of relaxation time (the first two terms of **Equation 3**);
[b] Result of fitting the temperature dependence of relaxation time using all terms of **Equation 3** in manuscript.

References to Electronic supplementary information

[S1] G. Socrates, *Infrared Characteristic Group Frequencies: Tables and Charts, 2nd Edition*, John Wiley & Sons, Chichester, England, **1994**.

[S2] M. Llunell, D. Casanova, J. Cirera, J. Bofill, P. Alemany, S. Alvarez, M. Pinsky and D. Avnir, *SHAPE v. 2.1. Program for the Calculation of Continuous Shape Measures of Polygonal and Polyhedral Molecular Fragments*, University of Barcelona: Barcelona, Spain, 2013.

[S3] D. Casanova, J. Cirera, M. Llunell, P. Alemany, D. Avnir and S. Alvarez, *J. Am. Chem. Soc.*, 2004, **126**, 1755.